

Short Report

Capturing colorectal cancer inter-tumor heterogeneity in patient-derived xenograft (PDX) models

Pramudita R. Prasetyanti^{1,2}, Sander R. van Hooff^{1,2}, Tessa van Herwaarden^{1,2}, Nathalie de Vries^{1,2}, Kieshen Kalloe^{1,2}, Hans Rodermond^{1,2}, Ronald van Leersum^{1,2}, Joan H. de Jong^{1,2}, Marek Franitza³, Peter Nürnberg³, Matilde Todaro⁴, Giorgio Stassi⁵ and Jan Paul Medema^{1,2}

¹Laboratory for Experimental Oncology and Radiobiology (LEXOR), Center for Experimental Molecular Medicine (CEMM) and Cancer Center Amsterdam, Academic Medical Center, Amsterdam, The Netherlands

²Oncode Institute, Academic Medical Center, Amsterdam, The Netherlands

³Cologne Center for Genomics (CCG), University of Cologne, Cologne, Germany Cologne Excellence Cluster on Cellular Stress Responses in Aging-Associated Diseases (CECAD), Cologne, Germany

⁴DIBIMIS, University of Palermo, Palermo, Italy

⁵Cellular and Molecular Pathophysiology Laboratory, Department of Surgical, Oncological and Stomatological Sciences, University of Palermo, Palermo, Italy

Patient-derived xenograft (PDX) models have become an important asset in translational cancer research. However, to provide a robust preclinical platform, PDXs need to accommodate the tumor heterogeneity that is observed in patients. Colorectal cancer (CRC) can be stratified into four consensus molecular subtypes (CMS) with distinct biological and clinical features. Surprisingly, using a set of CRC patients, we revealed the partial representation of tumor heterogeneity in PDX models. The epithelial subtypes, the largest subgroups of CRC subtype, were very ineffective in establishing PDXs, indicating the need for further optimization to develop an effective personalized therapeutic approach to CRC. Moreover, we showed that tumor cell proliferation was associated with successful PDX establishment and able to distinguish patient with poor clinical outcomes within CMS2 group.

Only ~7% of new cancer drugs entering phase I clinical trial gain market approval, mainly due to the lack of efficacy and robust preclinical data.^{1,2} This high failure rate underscores

Key words: colorectal cancer, cell proliferation, xenograft, CMS, tumor subtype, PDX

Additional Supporting Information may be found in the online version of this article.

P.R.P. and S.R.H. contributed equally to this work

Grant sponsor: AIRC 5x1000 ; **Grant numbers:** 9979; **Grant sponsor:** Dutch Cancer Society ; **Grant numbers:** 2009-4416, 2012-5735, 10150 and 10651 to J.P.M.; **Grant sponsor:** Gravitation program ZonMW; **Grant sponsor:** Koningin Wilhemina Fonds; **Grant numbers:** MLDS FP13-07 to J.P.M

This is an open access article under the terms of the Creative Commons Attribution-NonCommercial License, which permits use, distribution and reproduction in any medium, provided the original work is properly cited and is not used for commercial purposes.

DOI: 10.1002/ijc.31767

History: Received 22 Feb 2018; Accepted 9 Jul 2018; Online 27 Aug 2018

Correspondence to: Jan Paul Medema, Laboratory for Experimental Oncology and Radiobiology (LEXOR), Center for Experimental Molecular Medicine (CEMM) and Cancer Center Amsterdam, Academic Medical Center, Meibergdreef 9, Room G2-131, Amsterdam 1105AZ, The Netherlands, Tel.: +31-20-5667777; Fax: +31-20-6977192, E-mail: j.p.medema@amc.uva.nl

the need for more clinically predictive models. Directly isolated from cancer patients and transplanted into mice, patient-derived xenografts (PDXs) have the potential to fill this gap. In this role, PDXs have been used to identify novel therapeutic targets and resistance biomarkers that cell lines failed to capture.³⁻⁵ Accordingly, PDXs are advocated as reliable avatars of individual tumors by faithfully recapitulating the biological characteristics and genetic heterogeneity within tumors.^{6,7} However, it remains an open question as to what extent PDXs represent the heterogeneity observed between patients, which is especially relevant when considering the fact that not all tumors can successfully generate a PDX. Colorectal cancer (CRC) is a heterogeneous disease that can be stratified into four consensus molecular subtypes (CMS) with distinct biological features and clinical outcomes.⁸ CMS stratification has the potential to transform CRC treatment by matching drug efficacy with cancer subtype.⁹ To achieve this goal, it is essential to recapitulate patient subtypes in preclinical models. We, therefore, explored the factors contributing to successful PDX establishment in CRC and particularly examined whether all subtypes are adequately represented in PDXs.

We subcutaneously implanted 42 surgically resected tumors into immune-deficient mice (Fig. 1a, Supporting Information Fig. S1a). These tumors represented CRC diversity in terms of patient characteristics, such as stage, size, and

What's new?

Patient-derived xenograft (PDX) models have become an important asset in translational cancer research. However, colorectal cancer (CRC) can be stratified into four consensus molecular subtypes (CMS) with distinct biological and clinical features, and to what extent the existing CRC PDX collection represents the inter-patient heterogeneity remains an open question. This study identifies a subtype-specific bias in the establishment of PDXs from CRC patients, leaving the major subtype CMS2 strongly underrepresented. Additionally, the findings suggest that further classification within CMS can be achieved. For CMS2, the proliferation-related marker Ki67 may thus help refine patient classification, estimate prognosis, and guide treatment decisions.

CMS (Fig. 1*b*, Supporting Information Table S1). We achieved a PDX take rate of 52% (22% total, 10% primary, and 12% metastatic lesions), which is slightly lower as compared to a previous PDX study using the same mouse strain (63.5%).⁷ Occasional lymphoma formation was detected (7% of cases), likely representing outgrowth of EBV+ B cells as previously described.¹⁰ Metastatic origin of the tumor was significantly associated with engraftment success (Fischer's exact test, $p = 0.028$), whereas none of the other clinicopathological and (epi)genetic parameters showed a significant correlation (Fig. 1*c*). Comparison between PDX models and their corresponding donors showed that PDX models retain patient histopathological and molecular features (Supporting Information Figs. S1*b*–S1*d*).

CMS classification was obtained for the patients for which expression data could be generated ($N = 34$). For 33 out of 34 patients, reliable classification was achieved and the subtype ratios were in accordance with the ratios previously described.⁸ Strikingly, when engraftment success was evaluated, CMS1 and CMS4 were shown to be more efficient than the epithelial subtypes CMS2 and CMS3 (Fig. 1*d*, left). This also holds when analyzing PDX establishment from primary tumor origin only (Fig. 1*d*, right), indicating that CMS2/3 cancers displayed a lower engraftment success. The enrichment toward CMS1 and CMS4 became even more prominent when considering the capacity to serially engraft for at least three passages. The large majority of CMS4 tumors (78%) reached passage three (F3), whereas CMS2 tumors, the largest subgroup in CRC, had a much lower efficacy (13%) (Fig. 1*e*). Similar to CMS2, only 20% of CMS3 tumors reached F3, whereas 75% of CMS1 engrafted successfully, suggesting an engraftment bias against the epithelial subtypes (CMS2 and CMS3). Here, it is also evident that the engraftment success as measured by propagation to passage 3 is significantly higher from metastases-derived samples as compared to primary samples. However, even within the metastasis group, we observe that only 1 in 4 CMS2 samples reached passage 3, whereas 6 out of 6 CMS4 samples were successfully engrafted. Consequently, CMS4- and CMS1-derived PDXs were overrepresented at later passages, increasing from 39% in the patient population to 77% of F3 PDX models (Fig. 1*f*). We did not observe a clear difference in growth speed across subtypes. As shown before,¹¹ growth speed accelerated with increased passaging (F2–F3) (Supporting Information Figs. S1*e* and S1*f*), which likely represents an adaptation to the xenotransplantation conditions. Both the subtype-specific PDX engraftment efficiency and the subsequent serial passaging

efficiency challenge the design of preclinical PDX trials. Traditionally, tumor pieces are transplanted into a limited number of mice to generate a PDX repository, which is then serially expanded into a large number of mice in order to create a sufficient statistical power to detect the differences between treated and control group.¹² Our study suggests that this typical design is not equally suitable for all tumor subtypes and selects against the most prevalent subtype CMS2, which cannot be efficiently propagated.

To further investigate the underpinnings of the differential engraftment potential, we compared gene expression from tumors with and without successful engraftment (Fig. 2*a*). Gene set enrichment analysis (GSEA) revealed that cell cycle activity/proliferation was significantly down-regulated in tumors with successful engraftment, suggesting that tumors with high proliferative capacity failed to engraft (Fig. 2*b* and 2*c*). This difference was also evident in tumors that managed to propagate until F3 (Supporting Information Fig. S1*g*). To confirm this, the level of the cell cycle-related protein Ki67¹³ was measured. Consistent with the gene expression analysis, the number of Ki67⁺ cells was negatively correlated with engraftment success (Figs. 2*d* and 2*e*). This is in line with the observation that CMS2 cancers, which engraft poorly, display high cell cycle-related gene expression compared to CMS4 cancers.⁸ However, closer examination of Ki67 expression levels within CMS2 tumors showed that PDX establishment is not simply a corollary of differences between CMS2 and CMS4 tumors. In fact, it revealed that low tumor proliferation is a predictor of engraftment success in CMS2 cancers (Fig. 2*f*). As PDX establishment has been linked to patient outcome,¹⁴ we investigated whether this observation is clinically relevant and can be exploited to stratify patients. We found that low Ki67 gene expression was prognostic for recurrences when analyzing 741 stage II CRC patients (HR = 1.76, $p < 0.006$; Fig. 2*g*), but showed a much stronger, but also variable, prognostic value when analyzed per subgroup. Indeed, further segregation into distinct subtypes indicated that low Ki67 was not predictive for all subtypes. Although CMS1 and CMS4 patients did not show a significant association of Ki67 with recurrence, a strong prognostic effect was detected in CMS2 cancers, which had a higher propensity to recur when Ki67 was low (HR = 2.43, $p < 0.009$) (Fig. 2*h*). Surprisingly, the picture for CMS3 cancers showed the exact opposite, that is, positive correlation of Ki67 expression with recurrence (HR = 0.14, $p < 0.01$). Cell cycle activity is therefore an

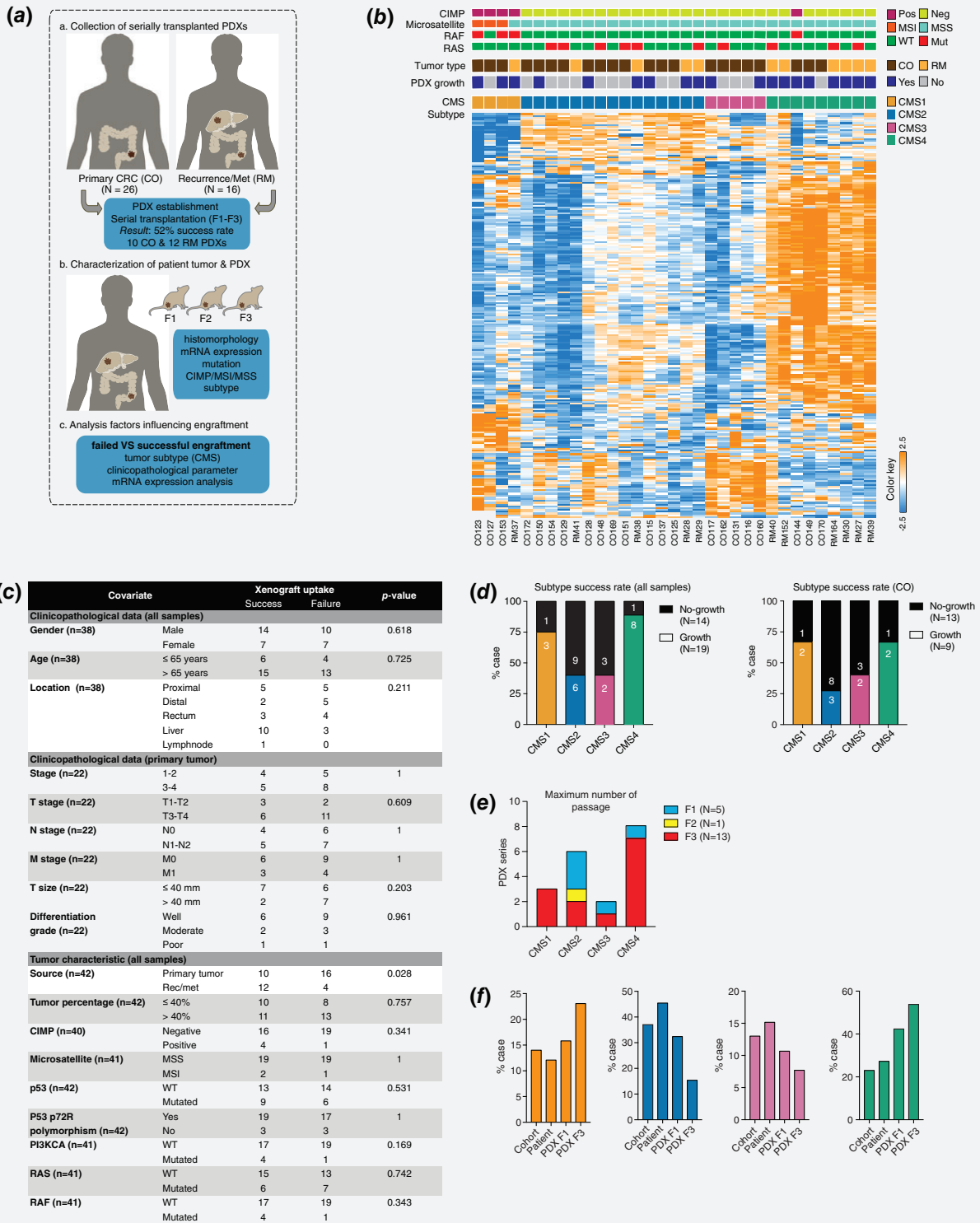


Figure 1. Establishment of PDX model. (a) Schematic of the pipeline employed in the establishment of PDX models. (b) Gene expression heatmap and corresponding genetic profile of tumors used to establish PDX. (c) Association of patients' characteristic with engraftment success. (d) CMS1 and CMS4 were associated with engraftment success compared to CMS2/3. Figures shown is CMS distribution in all samples (left) and primary tumors (right). (e) Detailed evaluation for each subtypes revealed that CMS1 and CMS4 could be efficiently passed until third passage while most of CMS2/3 tumors could not pass the second round of passage. (f) Comparison of subtype ratios between reported patient cohort,⁸ patient in our study and the corresponding rounds of passage showed enrichment of CMS1 and CMS4 with increasing passage number. [Color figure can be viewed at wileyonlinelibrary.com]

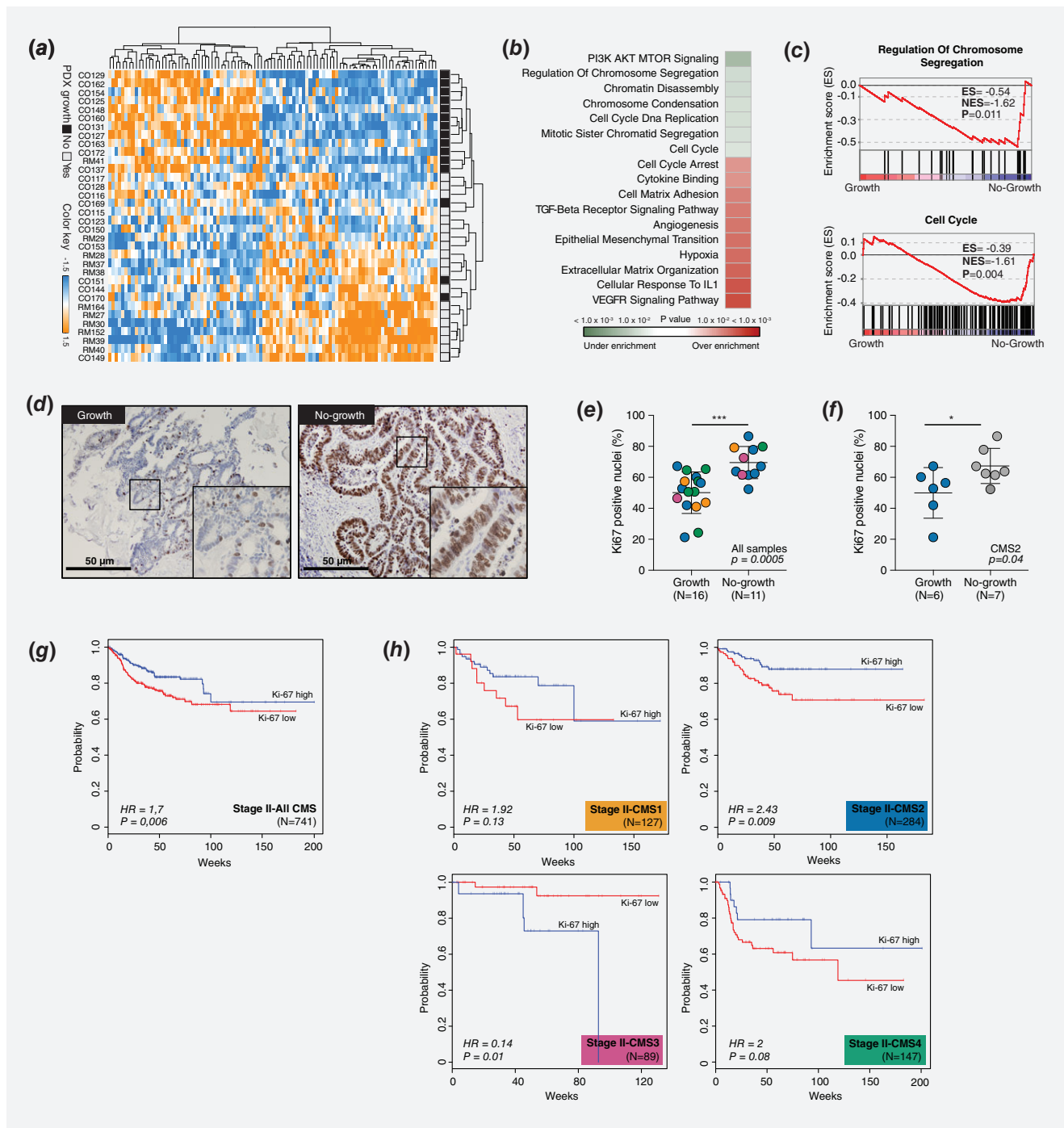


Figure 2. Proliferation status predicts the PDX engraftment and further refines CMS2 classification. (a) Heatmap showing genes differentially expressed between tumors with and without successful engraftment. (b, c) GSEA analysis of tumors with successful engraftment confirmed a negative association with cell proliferation related pathways. (d) Ki67 staining from patient's section. Positive antibody signals in the nuclei are shown in brown. (e) The mean of Ki67-positive nuclei between tumor with positive and negative engraftment was 50% and 71%, respectively. (f) The mean of Ki67-positive nuclei between CMS2 tumor with positive and negative engraftment was 50% and 67%, respectively. Statistics in (e) and (f) was performed with *t*-test. (g) Kaplan–Meier recurrence-free survival analysis on stage II patients as a group or (h) per CMS showed that the association of Ki67 expression with prognosis was subtype-specific. *p* value is calculated with the log-rank test. HR, hazard ratio. [Color figure can be viewed at wileyonlinelibrary.com]

important prognostic factor, but it should be used with caution and in a subtype-specific manner. Heterogeneity of clinical outcome within subtype was previously suggested when

analyzing the oxaliplatin response in patients¹⁵ and may provide the first hint that further stratification within a given subtype may be clinically relevant.

Altogether our current study identifies a subtype-specific bias in the establishment of PDXs from CRC patients, leaving the major subtype (CMS2) is strongly underrepresented. Drug efficacy studies aimed at this subtype are therefore unlikely to provide useful insight when an unselected set of PDX models is used. Consequently, optimization in PDX establishment is necessary to capture all tumor types. Combined with careful selection of the proper PDXs, these efforts will ultimately improve drug development strategies. Importantly, our PDX models did reveal a surprising relation between proliferation and recurrence rate specifically within CMS2, indicating that CMS2 may not be a homogeneous subtype and can be further refined. The relevance is further strengthened when considering that the CMS2 cancers that do engraft appear to be associated with poor clinical outcome.

Material and Method

Tissue processing

All tumor specimens (CO and RM) were obtained from patients that underwent routine surgery in two medical centers: Academic Medical Centre (AMC, Amsterdam, the Netherlands) and Flevo Hospital (Almere, the Netherlands). Samples were processed in accordance with the rules and legislation in the Netherlands and approved by the Medical Ethical Committee of the AMC immediately after surgery (ranging between 1 and 3 hr).

Engraftment procedure

Subcutaneous implantation was performed on one flank of 6–8 week-old athymic nude mice (Harlan laboratories) or (NSG) mice weighing from 18 to 25 g that were anesthetized by a mixture of isoflurane/oxygen. Tumor growth was monitored by bi-weekly measurements of the implantation sites. The serial engraftments of each tumor were conducted when the tumors reached a volume of 200–1,000 mm³. Animals were housed in IVC cages at the Animal Research Institute Amsterdam (ARIA-IWO), and all animal experiments were carried out under protocols approved by the Animal Ethical Committee of the AMC.

Characterization of patient tumors and corresponding PDX model

Immunohistochemistry. Hematoxylin–eosin (Sigma) and alcian blue according to the protocol from the manufacturer. Ki67 antibody was used (ab15580; dilution 1:5,000; Abcam, Cambridge, United Kingdom) as previously described.¹⁶ Ki-67 percentage was defined as the percentage of tumor nuclei showing Ki-67 staining per total of neoplastic cells counted in three randomly selected fields of tumor.

Genetic analysis and sample identification. DNA and RNA isolation, microsatellite stability status, CIMP, *KRAS*, *p53*, and *BRAF* mutation status were analyzed as described before.¹⁷ Only samples with a tumor epithelial area above 20% were

used for DNA and RNA extraction. Detection of *NRAS* and *PI3KCA* mutations (specifically E542K, E545G, E545K, and H1047R) was performed as previously described.¹⁸ To confirm that the material derived from PDX models originated from the corresponding patient tumor, we assessed two polymorphic pentanucleotide markers (Penta C and Penta D) for sample identification.

Microarray data generation. Samples with RNA integrity numbers ≥ 7 and A260/A280 ratio of ≥ 1.8 were included in the microarray analysis. Hybridization was performed on 34 patients and 37 PDX models using the GeneTitan MC (Affymetrix, Santa Clara, CA) according to the standard protocol of the Cologne Center for Genomics (CCG), University of Cologne, Germany. The microarray data were normalized, summarized, and log₂ transformed using robust multiarray analysis and batch effects were removed using Combat as implemented in the sva package (version 3.22.0). All normalization and batch effect correction was done separately for data derived from patients and PDX models. After normalization the probesets were annotated using the hgu133plus2.db annotation package (version 63).¹⁹ In case of multiple probesets interrogating a specific gene, the probeset with the highest mean intensity was selected as representative for that gene. The data set has been deposited in the Gene Expression Omnibus (GEO) repository under the accession number GSE100480.

CMS stratification of CRC tumors. The patient tumors were CMS stratified using a support vector machine (SVM) classifier trained on a data set of 466 CMS stratified CRC tumors (GSE39582). The expression data for GSE39582 were downloaded from the NCBI GEO gene expression repository and the data were normalized, batch corrected, and annotated as described earlier in the section. CMS labels for the tumor samples were obtained from Guinney *et al.*⁸ Only genes with sufficient variation (standard deviation > 0.25) were included in the next step where the most relevant genes were selected for the final classifier construction (i.e., feature selection). This selection was performed using iterative resampling (without replacement) where 80% of CMS classified samples were randomly selected and used to identify the top100 genes that were most differentially expressed in one CMS class *versus* the other three CMS classes. Differential expression was determined using the limma R package²⁰ and gene ranking was done on Benjamini-Hochberg corrected *p* values. Doing this for all four CMS classes resulted in 400 selected genes per iteration. After 1,000 iterations, we retained genes that were selected in at least 250 iterations for final classifier construction (450 genes) and used those genes to construct a SVM classifier (e1071 R package, version 1.6-8)²¹ with all 466 CMS stratified samples in GSE39582. Tumor samples with a classification probability >0.5 were assigned a CMS label (33 of 34 tumors, 97%).

Correlation analysis. For the correlation analysis, genes were selected that showed similar expression patterns in patient tumors and PDX models using the correlation of correlation approach.⁸ All genes with a correlation of correlations coefficient >0.25 were selected for further analysis. For the correlation analysis, 1,000 genes were selected that showed the highest standard deviation in the PDX samples to ensure sufficient variation. After gene-wise mean-centering is done separately for patient tumors and PDX tumors, the Pearson correlation between samples was calculated.

Gene set enrichment analysis (GSEA). GSEA was performed using a selection of genesets (c5.bp.v5.1.entrez.gmt) from MSigDB (<http://www.broadinstitute.org/gsea/>) release 5.1.²² The analysis was done using the GSA procedure with 10,000 permutations as implemented in the GSA R package (version

1.03). Enrichment score plots were made with the GSEA desktop application.

Ki67 stratification. The Ki67 stratification was done using the median expression of Ki67 (MKI67). Samples with an expression level \geq median expression were assigned to the Ki67 high group, those with an expression < median expression to the Ki67 low group. The survival distributions for the groups were compared to the log-rank test tumor subtypes.

Acknowledgments

The authors express sincere thanks to the physicians who have performed surgeries (P.J. Tanis, W.A. Bemelman, C.J. Buskens). The authors also thank R. Kandimalla for his technical assistance in the mutation analysis, R.D. Blok for his assistance in the data collection and M.F. Bijlsma for his helpful comments.

References

- Hay M, Thomas DW, Craighead JL, et al. Clinical development success rates for investigational drugs. *Nat Biotechnol* 2014;32(1):40–51.
- Seruga B, Ocana A, Amir E, et al. Failures in phase III: causes and consequences. *Clin Cancer Res* 2015;21(20):4552–60.
- Gao H, Korn JM, S F, et al. High-throughput screening using patient-derived tumor xenografts to predict clinical trial drug response. *Nat Med* 2015;21(11):1318–25.
- Bertotti A, Migliardi G, Galimi F, et al. A molecularly annotated platform of patient-derived xenografts (“xenopatients”) identifies HER2 as an effective therapeutic target in cetuximab-resistant colorectal cancer. *Cancer Discov* 2011;1(6):508–23.
- Zanella ER, Galimi F, Sassi F, et al. IGF2 is an actionable target that identifies a distinct subpopulation of colorectal cancer patients with marginal response to anti-EGFR therapies. *Sci Transl Med* 2015;7(272):272ra12.
- Hidalgo M, Amant F, Biankin AV, et al. Patient-derived Xenograft models: an emerging platform for translational cancer research. *Cancer Discov* 2014;4(9):998–1013.
- Julien S, Merino-Trigo A, Lacroix L, Pocard M, Goéré D, Mariani P, et al. Characterization of a large panel of patient-derived tumor xenografts representing the clinical heterogeneity of human colorectal cancer. *Clin Cancer Res*. 2012;18(19):5314–28.
- Guinney J, Dienstmann R, Wang X, et al. The consensus molecular subtypes of colorectal cancer. *Nat Med* 2015;21(11):1350–6.
- Linnekamp JF, Wang X, Medema JP, et al. Colorectal cancer heterogeneity and targeted therapy: a case for molecular disease subtypes. *Cancer Res* 2015;75(2):245–9.
- Dieter SM, Giessler KM, Kriegsmann M, et al. Patient-derived xenografts of gastrointestinal cancers are susceptible to rapid and delayed B-lymphoproliferation. *Int J Cancer* 2017;140(6):1356–63.
- Pearson AT, Finkel KA, Warner KA, et al. Patient-derived xenograft (PDX) tumors increase growth rate with time. *Oncotarget* 2016;7(7):7993–8005.
- Bertotti A, Migliardi G, Galimi F, et al. A molecularly annotated platform of patient-derived Xenografts (“Xenopatients”) identifies HER2 as an effective therapeutic target in Cetuximab-resistant colorectal cancer. *Cancer Discov* 2011;1(6):508 LP–23.
- Gerdes J, Lemke H, Baisch H, et al. Cell cycle analysis of a cell proliferation-associated human nuclear antigen defined by the monoclonal antibody Ki-67. *J Immunol* 1984;133(4):1710–5.
- Young Oh B, Yong Lee W, Jung S, et al. Correlation between tumor engraftment in patient-derived xenograft models and clinical outcomes in colorectal cancer patients. *Oncotarget* 2015;6(18):16059–68.
- Song N, Pogue-Geile KL, Gavin PG, et al. Clinical outcome from Oxaliplatin treatment in stage II/III colon cancer according to intrinsic subtypes: secondary analysis of NSABP C-07/NRG oncology randomized clinical trial. *JAMA Oncol* 2016;2(9):1162–9.
- Zimberlin CD, Lancini C, Sno R, et al. HDAC1 and HDAC2 collectively regulate intestinal stem cell homeostasis. *FASEB J* 2015;29(5):2070–80.
- Melo FDSE, Wang X, Jansen M, et al. Poor-prognosis colon cancer is defined by a molecularly distinct subtype and develops from serrated precursor lesions. *Nat Med* 2013;19(5):614–8.
- Lurkin I, Stoehr R, Hurst CD, et al. Two multiplex assays that simultaneously identify 22 possible mutation sites in the KRAS, BRAF, NRAS and PIK3CA genes. *PLoS One* 2010;5(1):1–6.
- Carlson M. *org.Hs.eg.db: Genome wide annotation for Human*. R Package version 312. 2015.
- Ritchie ME, Phipson B, Wu D, et al. Limma powers differential expression analyses for RNA-sequencing and microarray studies. *Nucleic Acids Res* 2015;43(7):e47.
- Meyer D, Dimitriadou E, Hornik K, Weingessel A, Leisch F. *Misc functions of the Department of Statistics (e1071)*, TU Wien. R package version 1.6-2. 2014. <http://cran.r-project.org/package=e1071>
- Subramanian A, Tamayo P, Mootha VK, et al. Gene set enrichment analysis: a knowledge-based approach for interpreting genome-wide expression profiles. *Proc Natl Acad Sci U S A* 2005;102(43):15545–50.